AIN SHAMS UNIVERSITY FACULTY OF ENGINEERING	Vol. 38, No. 4, December 31, 2003	**SCIENTIFIC BULLETIN** ***Received on :2/10/2003*** ***Accepted on :18/11/2003*** **pp.: 43-59**

AN INNOVATIVE STRUCTURAL SYSTEM FOR LARGE INGROUND RC STORAGE TANKS

OSAMA O. EL-MAHDY[1]

ABSTRACT

The purpose of this paper is to propose an innovative and efficient shear connection for large underground reinforced concrete storage tanks constructed by diaphragm walls and inverted lining or large-scale open caisson method where an extra-deep diaphragm wall is employed to prevent the inflow of ground water during construction. This connection has been introduced because of its potential advantages for both economy and safety. A general nonlinear finite element model to analyze the proposed shear connection is presented. To account for the varied material properties the analytical model is divided into concrete and steel elements. Two-dimensional isoparametric eight nodes quadrilateral plane stress elements having two degrees of freedom at each node are used to idealize both concrete and steel parts. The interface between concrete and steel elements is represented by special six nodes quadratic line gap elements having both normal and shear stiffness. The steel material is modeled using an elasto-perfectly plastic model with a Von Mises yield criterion. The concrete behavior under compression is modeled using an elasto-plastic model with a Drucker-Prager yield criterion and associated plasticity. The concrete in tension is modeled using a smeared cracking model with tension cut-off, tension softening and variable shear retention. The analytical results are compared well with the calculated ones using the principles of static and material properties. Furthermore, the simplified design equations for the proposed shear connections according to ECP'01 are given.

KEYWORDS: Inground Tanks; Reinforced Concrete; Shear Connectors; Nonlinear Analysis; Modeling.

الملخص العربي:

يزداد الدور الذي تلعبه مواد البترول الخام والغاز الطبيعي المسال وغاز البترول المسال في السوق العالمي للطاقة, لذلك فانه في كثير من الدول يتم إنشاء خزانات ضخمة قد تصل سعة الواحد منها إلى200000م3 وذلك لتخزين هذه المنتجات البترولية بهدف الحفاظ على مصادر للطاقة طويلة المدى،

[1] Associate Professor, Department of Civil Engineering, Faculty of Engineering at Shoubra, The University of Zagazig, Cairo 11629, EGYPT.

وغالبا ما تكون هذه الخزانات إما تحت أو فوق الأرض، ويتعرض هذا البحث لهذه النوعية من الخزانات والتي يتم تنفيذها تحت الأرض باستخدام حائط مستمر عميق (دايافرام) وذلك لمنع تدفق المياه الجوفية أثناء التنفيذ، وفى هذا البحث تم اقتراح وصلة جديدة للقص بين حائط الخزان والدايافرام وذلك بهدف الاستفادة الدائمة من الدايافرام فى مقاومة حالة عدم الاستقرار (الطفو) وأيضا في مقاومة الضغط الجانبي على حوائط الخزان وبالتالي التقليل من التكلفة الإجمالية لهذه الخزانات، وقد تم استخدام طريقة العناصر المحددة والتحليل اللاخطى لنموذج مكون من الحديد والخرسانة يمثل الوصلة المقترحة، وقد تم تمثيل كلا من الحديد والخرسانة سواء في الضغط أو الشد بشكل دقيق وأيضا تم استخدام عناصر الالتصاق لتمثيل سطح التماس بين الحديد والخرسانة وقد تم دراسة نتائج الدراسة التحليلية من حيث الاجهادات الرئيسية وشكل التشكلات والشروخ المتولدة وأيضا مناطق الانهيار، أيضا تم حساب مقاومة الوصلة المقترحة باستخدام المعادلات المقترحة بواسطة باحثون آخرون وتم مقارنتها بنتائج الدراسة التحليلية ومن هذه المقارنة تم استنتاج أن النموذج المقترح يمثل هذه الوصلة بدقة تامة وبالتالي يمكن الاعتماد على النموذج التحليلي اللاخطى في التعرف على سلوك وصلة القص المقترحة، و أخيرا في هذا البحث تم تقديم المعادلات التصميمية المطلوبة لتصميم وصلة القص المقترحة وذلك طبقا للكود المصري لتصميم وتنفيذ المنشآت الخرسانية 2001م

1. INTRODUCTION

The role of crude oil, liquefied natural gas (LNG), and liquefied petroleum gas (LPG) in the world energy market are becoming more and more significant year by year. In this situation, in many countries, it is likely that large reinforced concrete storage tanks will be built so as to secure a stable long-term supply and increase diversity of energy sources. These storage tanks are now existing throughout the world and they may be classified according to their structural features into inground and above-ground tanks. The completely buried underground storage tanks present minimal disruption of surrounding landscape because the great bulk of the tanks are below the ground level. Therefore, several inground tanks have been built and are in operation from 1970 up to the present time. As an example, the world's largest LNG inground storage tank that was constructed in Japan in 1996 with an inner diameter of 68,130 mm and a liquid depth of 55,100 mm (i.e. capacity of 200,000 m^3).

However, in an inground storage tank, the treatment of ground water both during construction and after completion is an important factor in deciding on the structure type, design conditions, and construction methods [1].

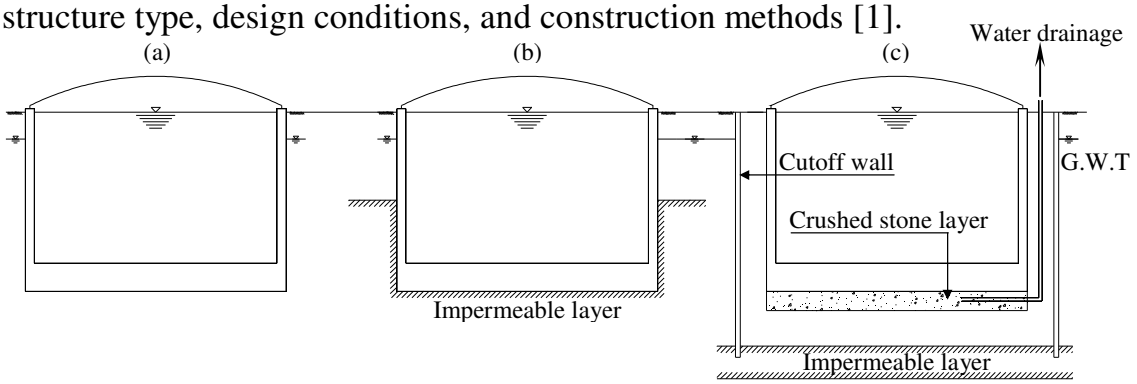

Fig. 1 Types of Inground Storage Tanks Classified by Methods of Groundwater Treatment

With respect to the ground water treatment method to be adopted after completion, the inground storage tanks can be classified into the following types (see Fig. 1): (a) A type in which uplift pressure due to the ground water acts on the underside of the base (Fig.1(a)); (b) A type in which the base is constructed on an impermeable layer and, when required, the seeping water is drained, so that no uplift pressure acts on the underside of the base (Fig. 1(b)); and (c) A type in which the ground water is cut off by an impermeable layer and a cut-off wall and the seeping water into the cut-off wall is drained so that the uplift pressure on the underside of the base is reduced (Fig. 1(c)).

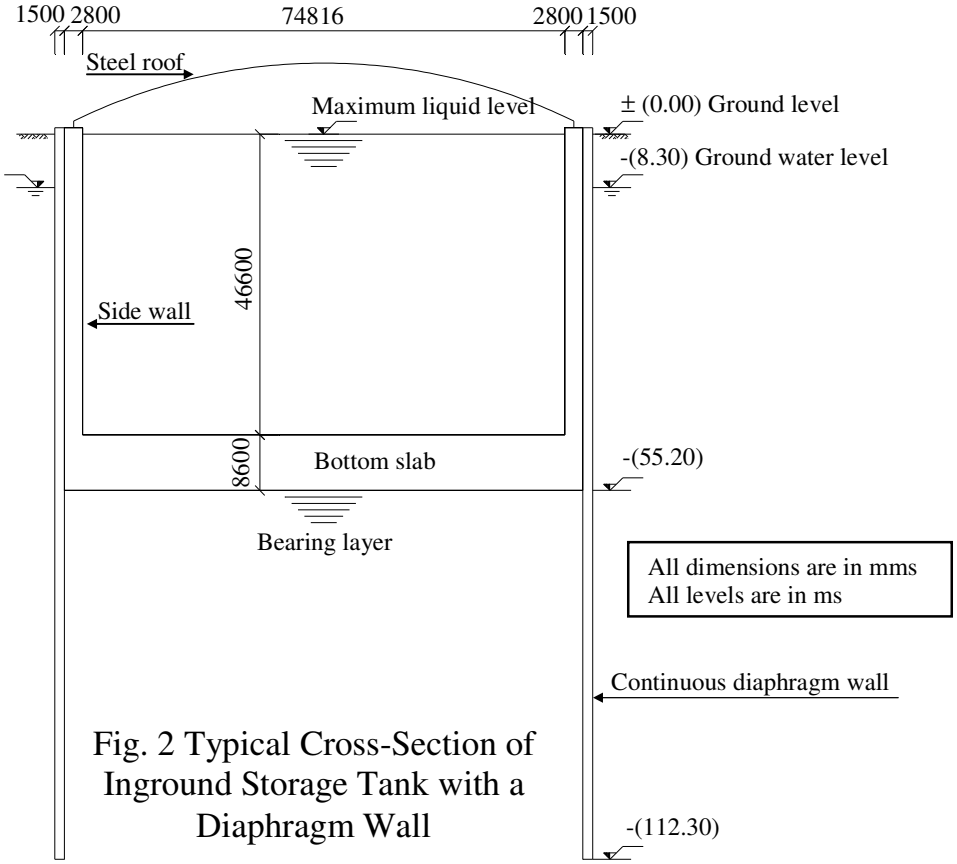

Fig. 2 Typical Cross-Section of Inground Storage Tank with a Diaphragm Wall

The present paper deals with type (a), in which the base slab resists the uplift pressure by its own dead weight or strength. Generally, this type of tanks is constructed by diaphragm wall and inverted lining or open caisson method where a deep diaphragm wall is employed to prevent the inflow of ground water during construction. Figure 2 shows a typical structural section for this type. In this research an innovative shear connection between the side wall of the inground tank and the diaphragm wall is developed. The details of the proposed shear connection are illustrated in Fig. 3. This type of connection has been introduced in order to increase the buoyant stability of the tank by utilizing both the counter weight and surface skin friction of the continuous diaphragm wall in resisting the ground uplift water pressure which acts on the base of the storage tank. Furthermore, the proposed connection helps in reducing the thickness of

tank side wall since the earth pressure, ground water pressure, liquid pressure, and loads caused by the earthquakes are resisted by both the tank side wall and the diaphragm wall. Therefore, this research work enables the designer to reduce the cost of construction and enhance the safety for such underground tanks.

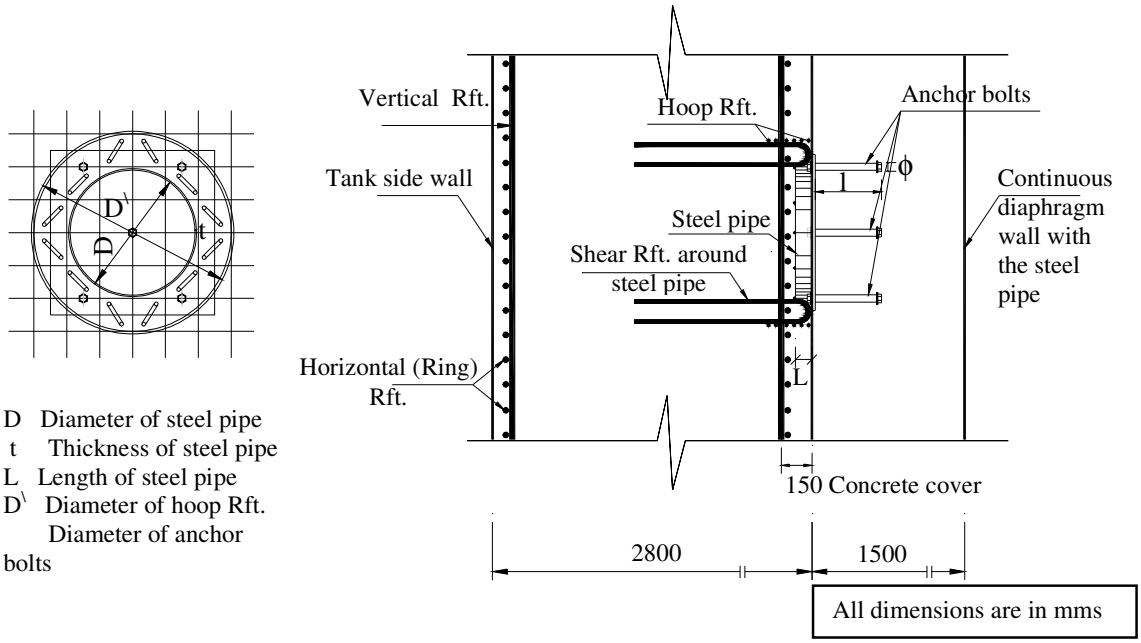

Fig. 3 Proposed Steel Pipes Shear Connections

The main objectives of this paper are: (1) to represent a simplified and efficient nonlinear finite element analytical model for the proposed shear connection; (2) to verify the applicability of the proposed model by comparing the predicted analytical results with the calculated ones obtained using the principles of static and material properties; and (3) to give the design equations for calculating the proposed shear connections in a simple, integrated and concise method. The following chapters of this paper are organized as follows. First, the nonlinear finite element model is presented. Next, the numerical technique is outlined. Then, the analytical results are presented followed by the discussion. After that, the simplified equations for the design of the proposed shear connections are given. Finally, the main conclusions of this work are withdrawn.

2. NONLINEAR FINITE ELEMENT MODELING

2.1 Finite Element Model

The finite element idealization of the proposed shear connection is shown in Fig. 4. The finite element mesh consists of 358 elements and 1111 nodes. To account for the varied material properties the analytical model is divided into concrete and steel elements.

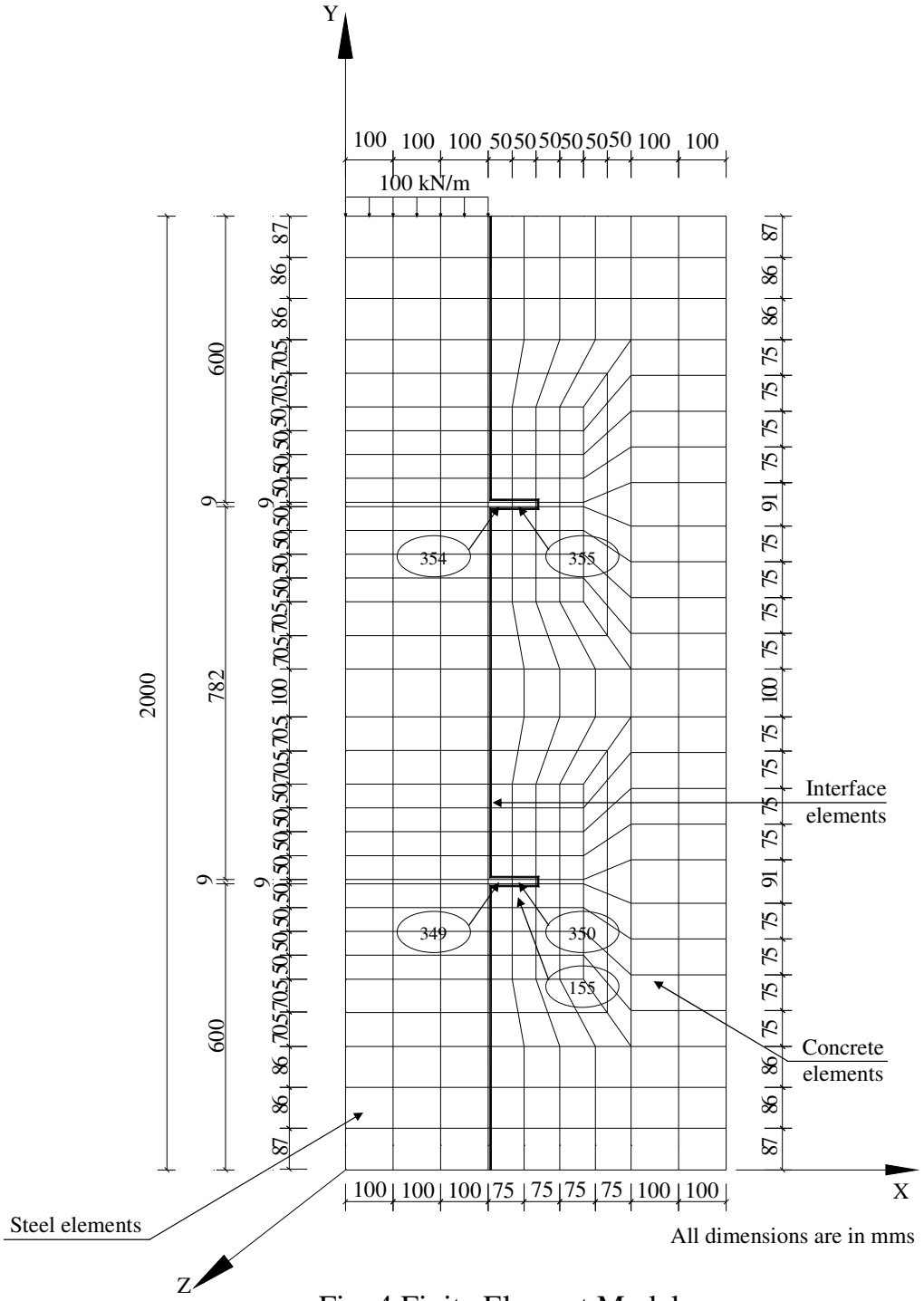

Fig. 4 Finite Element Model

Two-dimensional isoparametric eight nodes quadrilateral plane stress elements having two degrees of freedom at each node are used to idealize both concrete and steel parts (see Fig. 5). The interface between concrete and steel elements is represented by special six nodes quadratic line interface elements shown in Fig. 6. Each interface element contains two tractions, one acting parallel to the interface and the other acting perpendicular to it. The interface elements have no

physical dimensions and thus they are used to connect two separate nodes occupying the same physical position.

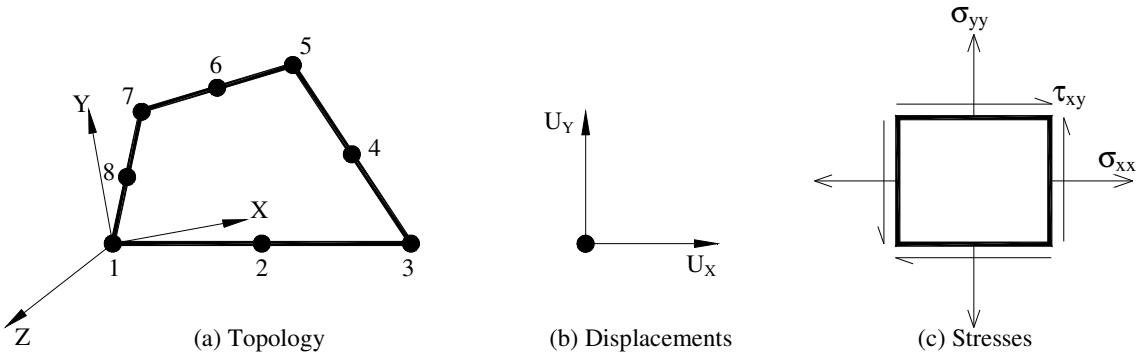

Fig. 5 Isoparametric Quadrilateral Plane Stress Element

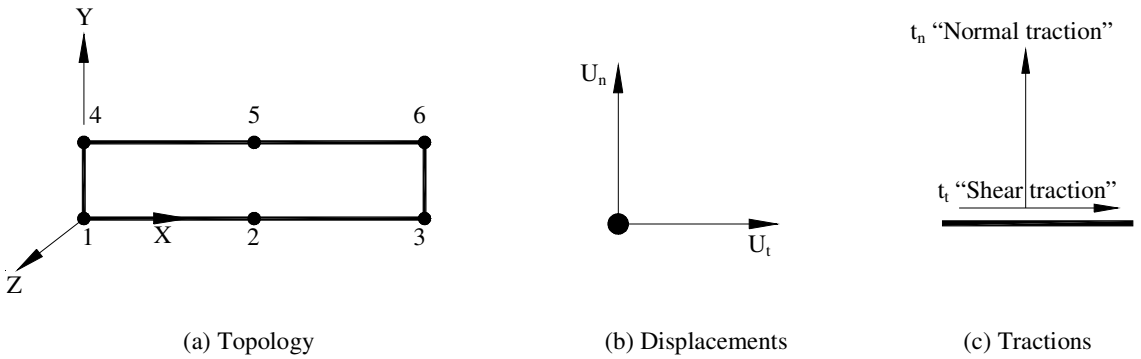

Fig. 6 Quadratic Line Interface Element

2.2 Material Idealization

The analytical model consists of concrete and steel materials. Therefore, realistic constitutive relationships for both materials should be used in calculations to obtain adequate accuracy. The aspects that are considered in the present nonlinear analysis are as follows: (a) tensile cracking and tension softening of concrete; (b) crushing of concrete in compression; and (c) yielding of steel. The following subsections are devoted to describe the nonlinear material modeling for concrete and steel elements. Further details about the used models are documented in [2] and [3].

2.2.1 Modeling of concrete

In compression, as shown in Fig. 7, the concrete is modeled by the equivalent uniaxial elasto-plastic model with Drucker-Prager's yield criterion. It should be noted that, the point of maximum compressive stress and strain (σ_p/ε_p) under

biaxial loading is a function of the principal stress ratio $\alpha=\sigma_1/\sigma_2$, the uniaxial compressive strength f_{cu}, and the strain at the peak uniaxial stress. Typical expressions for σ_p and ε_p are given in [3]. The surface of failure is expressed as follows:

$$F(I_1, J_2) = \alpha I_1 + \sqrt{J_2} - K = 0 \tag{1}$$

$$\alpha = \frac{\tan\varphi}{\sqrt{9 + 12\tan^2\varphi}} \qquad \text{and} \qquad K = \frac{3C}{\sqrt{9 + 12\tan^2\varphi}} \tag{2}$$

where I_1 is the hydrostatic component of the stress tensor σ_{ij}, J_2 is the second invariant of the deviatoric stress tensor s_{ij}, and α & K are the positive material constants which can be related to the friction angle φ and the cohesion C. For concrete the cohesion can be calculated from the following equation:

$$C = f_{cu}\frac{1 - \sin\varphi}{2\cos\varphi} \tag{3}$$

where f_{cu} is the characteristic compressive strength of concrete. If the concrete is crushed in compression at an integration point, all stresses then remain at the ultimate level while the stiffness matrix for the same integration point drops to a zero matrix. Furthermore, for simplicity the dilatancy angle ψ is assumed to be equal to the friction angle φ (i.e. associated flow rule).

In tension, the concrete material is modeled as a linearly elastic material with the inclusion of a descending branch in the stress-strain curve as illustrated in Fig. 8. A gross (or smeared) cracking concept was utilized, in which any cracking is assumed to be embedded, smeared over the tributary area (volume) of an entire integration point. After cracking has occurred (usually defined when the major principal tensile stress exceeds a tensile strength criterion for the concrete), the tangent modulus of elasticity is reduced to zero perpendicular to the principal tensile stress direction. Furthermore, in the direction parallel to the crack surface the shear modulus G with a reduction factor β is reinserted in the element constitutive matrix. Six possible crack configurations are included: (1) no crack; (2) one crack; (3) first crack closed; (4) first crack closed and second crack open; (5) both cracks closed; and (6) both cracks open. The incremental constitutive anisotropic tangent stiffness matrix for cracked concrete plane stress state is defined as follows:

$$\begin{Bmatrix} d\sigma_1 \\ d\sigma_2 \\ d\tau_{12} \end{Bmatrix} = \begin{bmatrix} 0 & 0 & 0 \\ 0 & Ec & 0 \\ 0 & 0 & \beta G \end{bmatrix} \begin{Bmatrix} d\varepsilon_1 \\ d\varepsilon_2 \\ d\gamma_{12} \end{Bmatrix} \tag{4}$$

in which E_c is the tangent modulus of concrete, the *1*-direction is perpendicular to the crack and *2*-direction is parallel to the crack.

Moreover, since the intact concrete between cracks is still capable of transferring some tensile stress, a descending branch for the tensile stress-strain curve of concrete was utilized in the present analysis (see Fig. 8). The use of this descending branch is often referred to as tension softening. Equation 5 gives the tension softening model which is used in this paper [4].

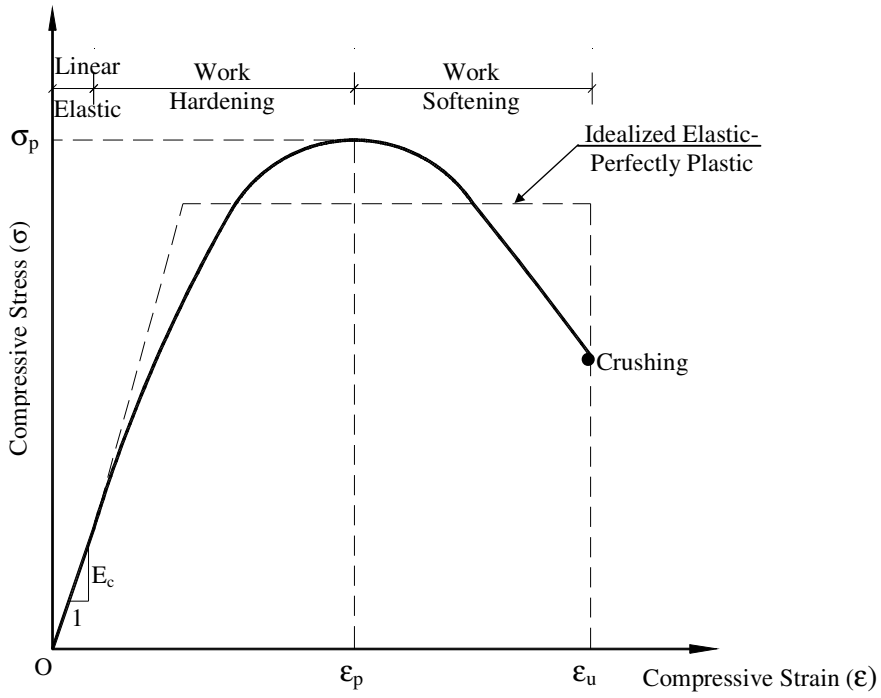

Fig.7 Equivalent Uniaxial Stress-Strain Curve for Concrete in Compression

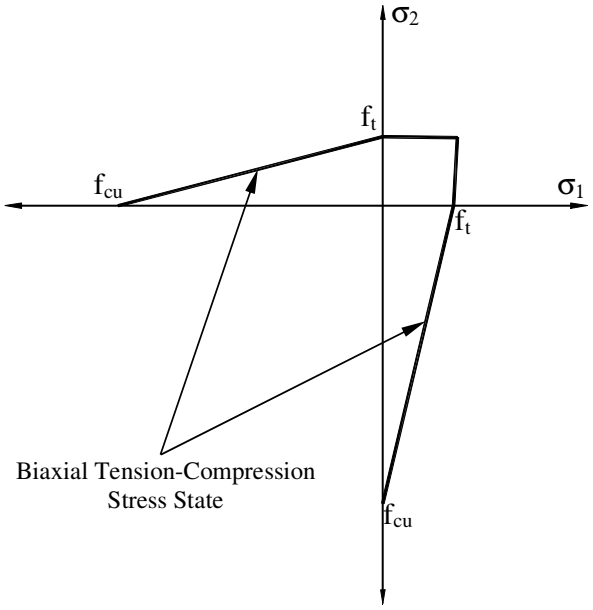

(a) Tension Cut-off in Two-Dimensional Principal Stress Space

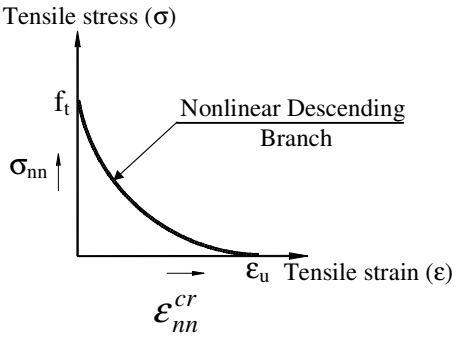

(b) Tension Softening Curve After Cracking

Fig.8 Cracking Criteria for Concrete

$$\frac{\sigma_{nn}}{f_t}=\left\{1+\left(c_1\frac{\varepsilon_{nn}^{cr}}{\varepsilon_u}\right)^3\right\}exp\left(-c_2\frac{\varepsilon_{nn}^{cr}}{\varepsilon_u}\right)-\frac{\varepsilon_{nn}^{cr}}{\varepsilon_u}\left(1+c_1^3\right)exp\left(-c_2\right) \quad (5)$$

with c_1=*3.0* and c_2=*6.93*. Where f_t is the concrete tensile strength, σ_{nn} is the tensile strength normal to the crack, ε_{nn}^{cr} is the tensile strain normal to the crack, and ε_u is the ultimate tensile strain.

2.2.2 Modeling of steel

Similar treatment as for concrete is proposed for steel. The steel material is idealized as an elastic-perfectly plastic model with a Von Mises yield criterion (i.e. the yielding begins when the octahedral shearing stress τ_{oct} reaches a critical value). Table 1 summarizes the various parameters used to describe the yield surfaces for concrete and steel.

Table 1 Various Parameters of the Yield Surfaces

Material Property	Material Type	
	Steel	Concrete
Yield Criterion	Von Mises	Drucker-Prager
Description of Yield Surface	Yield Stress	Cohesion, Friction Angle and Dilatancy Angle

2.2.3 Modeling of interface

The interface shear stiffness for all interface elements was assumed to be zero value. On the other hand, in order to simulate the bearing resistance of the concrete on the deformation of the steel plates, the normal stiffness for the interface elements number 349,350,354 and 355 was assumed equal to $1x10^8$ KN/m^3. The normal stiffness for all other interface elements was assumed to be zero.

2.3 Materials Properties

In the present analytical model, the material properties were taken as follows:

A. Concrete

Compressive strength	= 30 MPa
Tensile strength	= 3 MPa
Modulus of elasticity	= 20 GPa
Poisson's ratio	= 0.20

B. Steel

Yield stress	= 240 MPa
Modulus of elasticity	= 210 GPa
Poisson's ratio	= 0.30

3. NUMERICAL TECHNIQUE

A nonlinear analysis of the present model accounting for all important effects on internal stress distribution, crack propagation and external deformations can only be realized by a step-by-step solution procedure. Therefore, an incremental-iterative technique is utilized in the present analysis. This technique involves an incremental loading and two different iteration procedures to satisfy equilibrium and constitutive relations within each load increment.
The solution process starts with incrementation of the external loads. In each load increment the increments of nodal deformations and internal stresses are first obtained by using a global stiffness matrix containing tangential values of stiffness obtained in the previous load step. After computing the resulting stress and strain increments the total stresses of elements are not corresponding to the stress state obtained from constitutive relations for total strains. The "unbalanced" stresses are now integrated to get "unbalanced" nodal forces which are applied to the element nodes in the next iteration. In order to fully account for nonlinear material behavior an iterative technique is used as shown

in Fig.9 until satisfying the constitutive relations. It should be noted that the global stiffness matrix remains unchanged in this case.

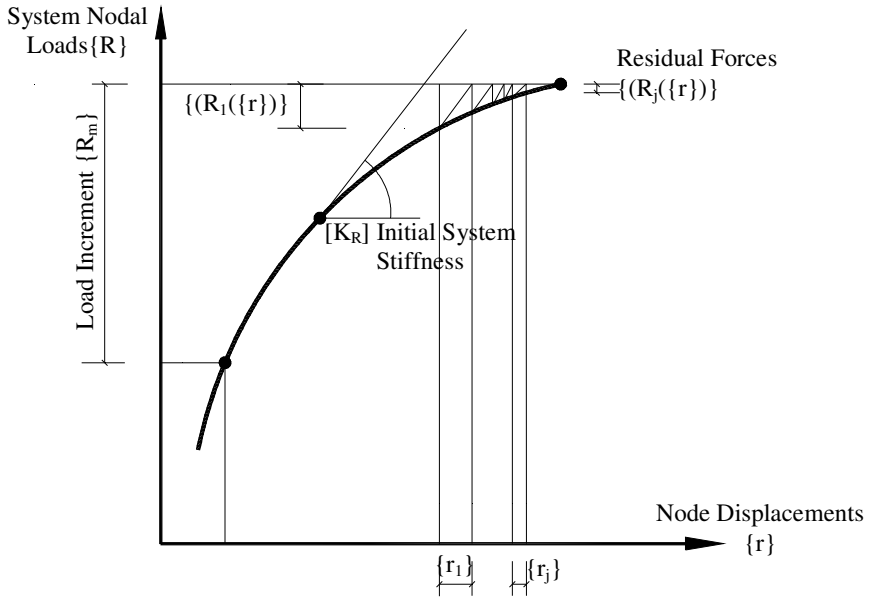

Fig. 9 Iterative Solution Procedure for Nonlinear Material Behavior

The analysis was carried out on a Sun/Sparc work station using the finite element program DIANA, version 8.0. The material is coded as a user-defined subroutine to the program. More information about DIANA may be found in [5].

4. ANALYTICAL RESULTS AND DISCUSSIOIN

First, a linear static analysis with an applied uniformly distributed load equal to 100 KN/m (see Fig. 4) was carried out in order to estimate the maximum stresses and to scale the first load-step for the nonlinear analysis. It should be noted that, the effect of self weight of the model was neglected in the analysis. Furthermore, at both right and left edges the displacements in the x-direction are suppressed and at the bottom edge of the concrete part the displacements in the y-direction are also restrained. From the obtained results, it can be seen that if the applied load is multiplied by 0.20, the tensile stress of element number 155 will just reach the cracking stress. Consequently, in the nonlinear analysis, the first two load steps were carried out using a 10 KN/m step for which the structure should still be completely linear, followed by 20 load steps each of 7.5 KN/m, then 10 load steps each of 4.5 KN/m until a total load of 215 KN/m is reached. After then, the analysis does not converge any more for further load steps, as the concrete elements are almost completely collapsed due to cracking.

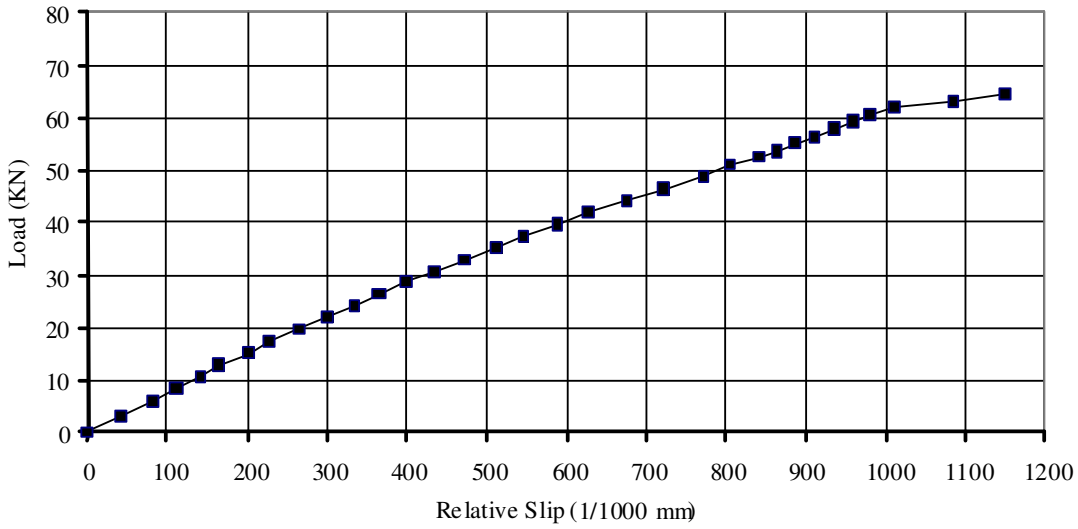

Fig. 10 Load-Relative Slip Relationship

Figure 10 shows the analytical load-relative slip relationship at node number 7 obtained from the load controlled analysis. In general, the shape of this curve is similar to that obtained from the push-out tests on headed studs shear connectors [6]. Furthermore, the ultimate strength of the shear connectors obtained from the present analytical model is 92% of that obtained from the well-known formula given by Ollgaard et al. [7].

The obtained principal stresses, deformed shape, plastic areas and cracking patterns at the last load step are illustrated in Figs. 11 to 14. From these figures, it can be concluded that the fracture of concrete occurred with two different configurations: (1) fracture which occurred when the principal stresses are either in tension-tension state or tension-compression state and their value exceeds the limit value; and (2) after then, the concrete is yielding when the principal stresses are in compression-compression state and their value exceeds the limit value (see Figs. 13 and 14). Moreover, the deformed shape, the cracking patterns and the modes of failure obtained from the present analytical model are identical to the findings of the experimental works on shear connectors that have been conducted by many researchers [8] and [9]. Consequently, it can be concluded that the proposed analytical model is accurate enough to simulate the nonlinear behavior of the proposed shear connections.

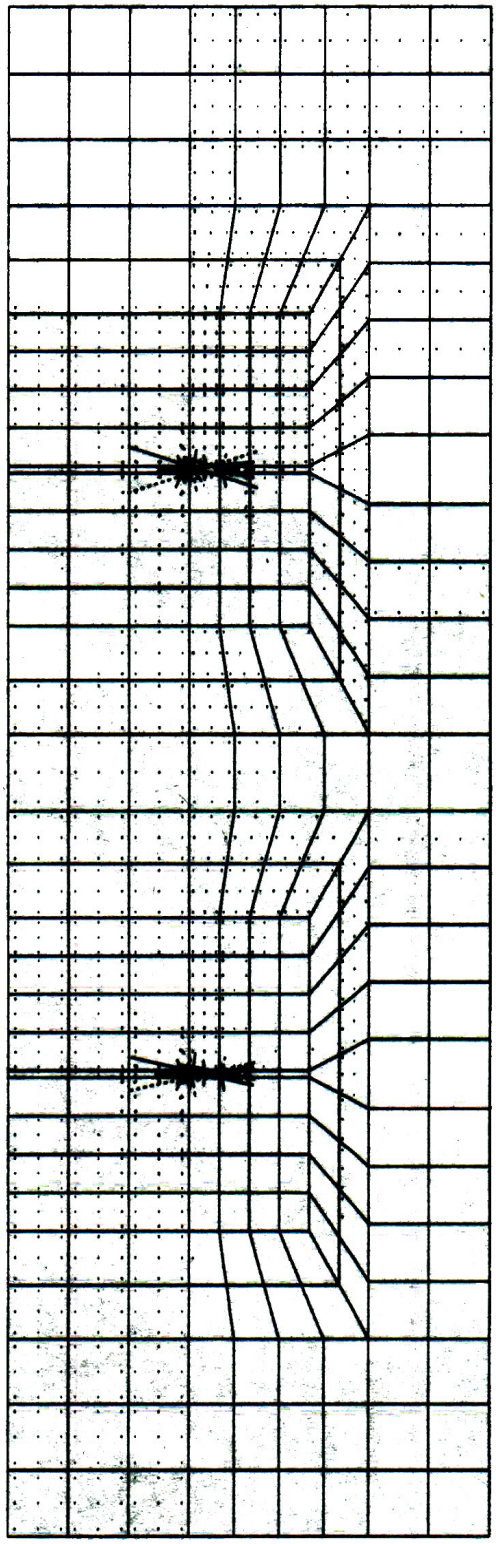

Fig. 11 Principal Stresses
at Load Step Number 32

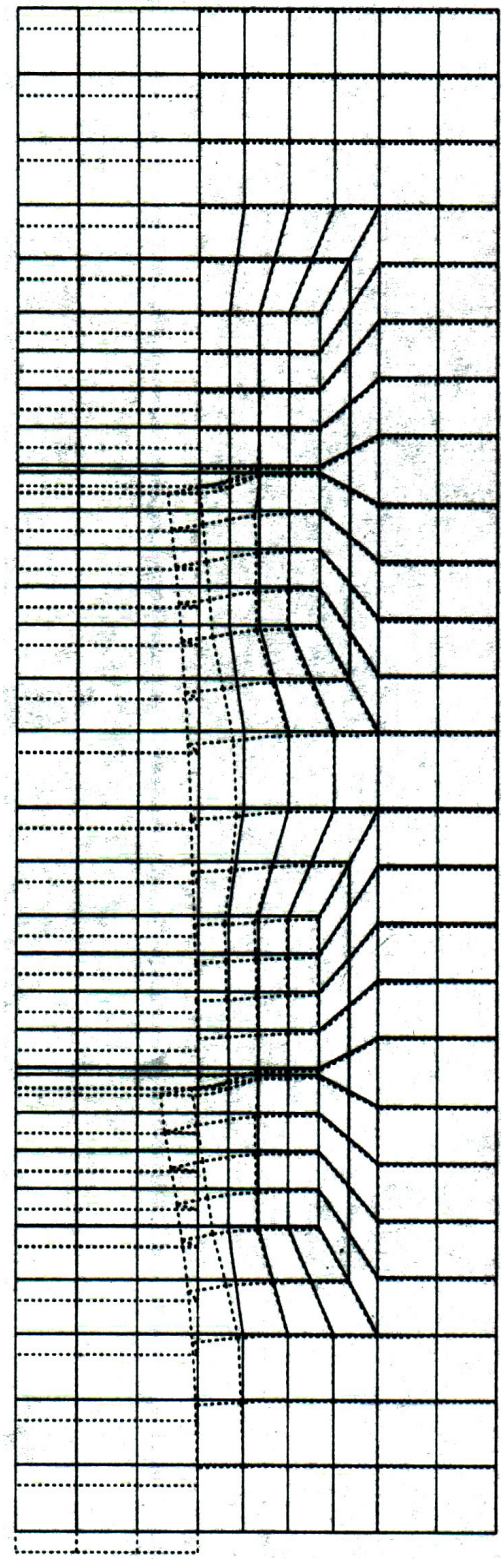

Fig.12 Deformed Shape
at Load Step Number 32

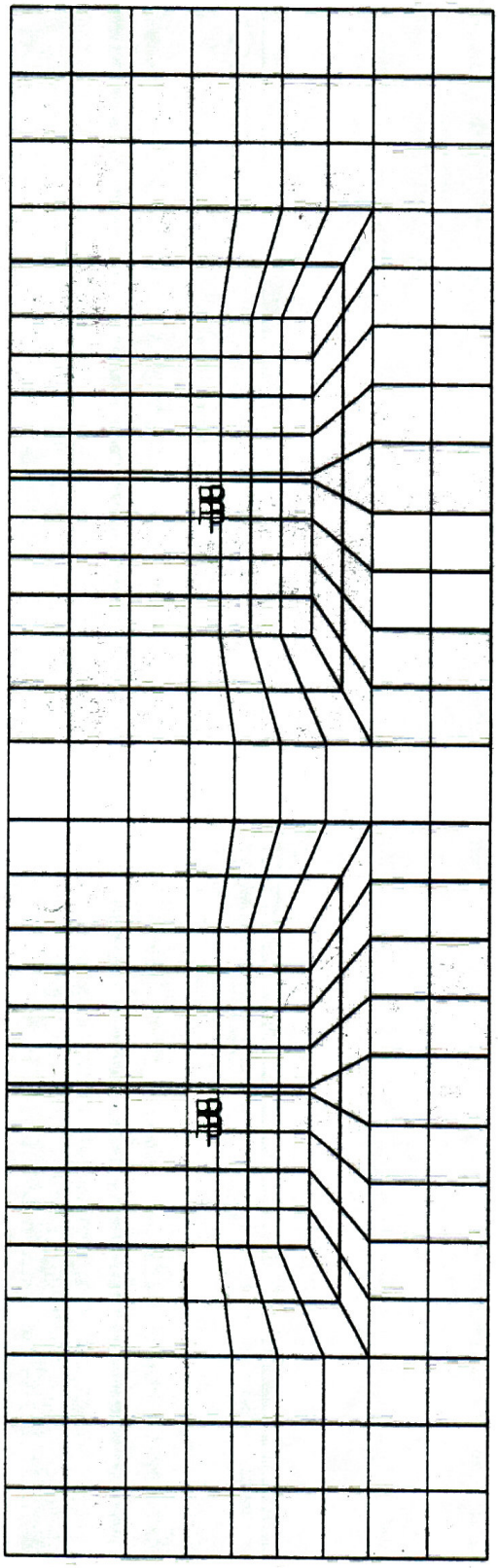

Fig. 13 Plastic Area at
Load Step Number 32

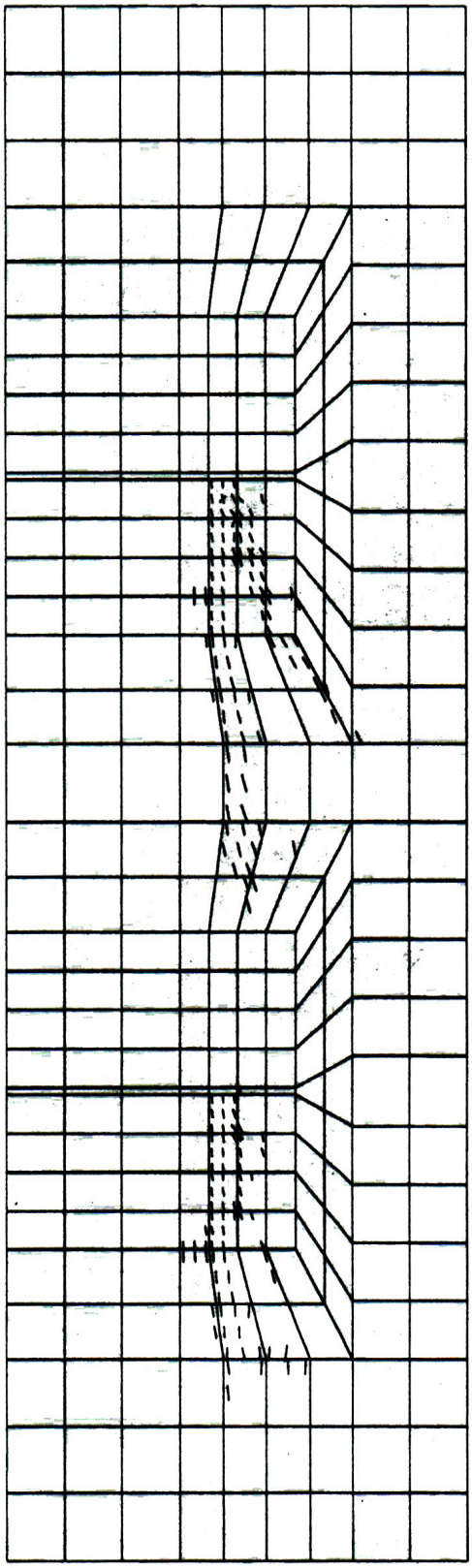

Fig. 14 Open Cracks Pattern
at Load Step Number 32

5. DESIGN OF THE PROPOSED SHEAR CONNECTION

In this section, the simplified design equations for the proposed shear connection are presented. In this sense, the present research covers the gab between the elaborate theoretical treatments of the connections on one hand, and, the practical aspects of the design of shear connectors, on the other hand. The following subsections summarize the required design equations as provided by ECP'01 [10].

(1) Ultimate Bearing Resistance of Steel Pipe (see Fig. 3)

$$P = 0.45 \times (D \times L) f_{cu} \tag{6}$$

where *DxL* is the bearing area and f_{cu} is the characteristic compressive strength of concrete.

(2) Calculation of Hoop Reinforcement

$$A_s = \frac{0.288P}{f_y} \tag{7}$$

where f_y is the yield stress for steel reinforcement.

(3) Calculation of Shear Reinforcement Around Steel Pipe

$$A_s = \frac{2.0P}{f_y} \tag{8}$$

(4) Calculation of Anchor Bolts

$$n = \frac{P}{A \times \tau_b} \tag{9}$$

where n is the number of anchor bolts, A is the cross-sectional area of the bolt, and τ_b is the ultimate shear strength of the bolt.

6. CONCLUSIONS

This research presents an innovative shear connection for large inground storage tanks constructed by diaphragm walls and inverted lining or open caisson

method. This connection is proposed to increase the stability of the tank by utilizing both counter weight and surface friction of the continuous diaphragm wall in resisting the ground uplift water pressure which acts on the base of the storage tank. Also, this connection helps to reduce the thickness of the tank side wall since the horizontal and vertical loads are resisted by both the side and diaphragm walls. A general nonlinear finite element model to analyze the proposed shear connection is presented. In the finite element model, two-dimensional isoparametric eight nodes quadrilateral plane stress elements having two degrees of freedom at each node are used to idealize both concrete and steel parts. Six nodes quadratic line gap elements having both normal and shear stiffness are used to model the interface between concrete and steel elements. The steel is modeled as an elasto-perfectly plastic material with a Von Mises yield criterion. The concrete behavior under compression is modeled using an elasto-plastic model with a Drucker-Prager yield criterion and associated plasticity. On the other hand, the concrete in tension is modeled using a smeared cracking model with tension cut-off, tension softening, and variable shear retention.

The load-relative slip relationship, cracking patterns, principal stresses, and plasticity areas can be obtained using the proposed analytical model. The obtained analytical results are compared well with both the calculated values and those obtained experimentally by other researchers . The comparison indicates that the proposed model is accurate enough to simulate the nonlinear behavior of the proposed shear connection. Also, simplified design equations for the proposed structural system are given.

REFERENCES

[1] Recommended Practice for LNG Inground Storage, (1979), Japan Gas Association Committee on LNG Inground Storage.

[2] ASCE Task Committee on Finite Element Analysis of Reinforced Concrete Structures, (1982), “State-of-the-Art Report on Finite Element Analysis of Reinforced Concrete”, American Society of Civil Engineers, New York.

[3] Chen, W.F., (1982), “Plasticity in Reinforced Concrete”, McGraw-Hill Book Company, New York.

[4] Reinhard, H.W., Cornelissen, H.A.W., and Hordijk, D.A., (1986), “Tensile Tests and Failure Analysis of Concrete”, Journal of Structural Engineering, Vol. 112, No. 11, pp. 2462-2477.

[5] DIANA - Finite Element Analysis User’s Manuals – Release 8.0, (2002). Published by TNO Building and Construction Research, Delft, The Netherlands.

[6] Kulak, G.L., Adams, P.F., and Gilmor, M.I., (1995), "Limit States design in Structural Steel", Canadian Institute of Steel Construction, Chapter 6, pp. 155-187.
[7] Ollgaard, J.G., Slutter, B.G. and Fisher, J.W., (1971), "Shear Strength of Stud Connectors in Lightweight and Normal-Weight Concrete", AISC Engineering Journal, Vol. 8, No.2, pp. 55-64.
[8] Evans, H.R. and Wright, H.D.,(1988),"Steel-Concrete Composite Structures: Stability and Strength", Chapter 2, pp.21-52, Edited by R.Narayanan, Elsevier Applied Science Publishers Ltd, U.S.A, ISBN 1-85166-134-4.
[9] Yam, L.C.P.,(1981),"Design of Composite Steel-Concrete Structures", Chapter 5, Published by Surrey University Press, U.K., ISBN 0-903384-22-1.
[10] ECP'01, (2001), "Egyptian Code of Practice for Design and Construction of Concrete Structures", Ministerial Decree No. 98-2001.